Environmentally benign synthesis of crystalline nanosized molecular sieves

Xiaoxin Chen, Guoju Yang, Valentin Valtchev

Environmentally benign synthesis of crystalline nanosized molecular sieves

Xiaoxin CHEN[1, ‡], Guoju YANG[1, 2, ‡], Valentin VALTCHEV[3,4 *]

[1]*State Key Laboratory of Inorganic Synthesis and Preparative Chemistry, College of Chemistry, Jilin University, Changchun 130012, Jilin, People's Republic of China.*

[2]*International Center of Future Science, Jilin University, Changchun 130012, Jilin, People's Republic of China.*

[3]*Qingdao Institute of Bioenergy and Bioprocess Technology, Chinese Academy of Sciences 189 Song Ling Rd Qingdao, Shandong 266101, P.R. China*

[4]*Normandie Univ, ENSICAEN, UNICAEN, CNRS, Laboratoire Catalyse et Spectrochimie, 6 Marechal Juin, 14050 Caen, France*

* **Corresponding author**. E-mail: valentin.valtchev@ensicaen.fr

‡ These authors contributed equally.

Abstract

Zeolites and zeo-type materials with nanosized dimensions are of great practical interest owing to their favorable transport properties, faster adsorption kinetics, and large external surface area. This mini-review presents recent developments in the organic template-free synthesis of nanosized zeolites and related materials. The advantages and challenges of these methods are addressed with particular attention to the green synthesis of nanozeolites.

Keywords: Zeolites; Organic template-free; Nanocrystals; Green synthesis.

1. Introduction

Inorganic microporous materials with uniform pores and cages, typically known as zeolites and zeo-type molecular sieves, have been widely studied due to their widespread applications in catalysis, gas adsorption/separation and ion-exchange [1-4]. Zeolite is a class of inorganic microporous material, whose structure consists of adjacent aluminium and silicon tetrahedron to form a three-dimensional (3D) framework with uniform pores of molecular dimensions [5]. Zeo-type molecular sieves contain different tetrahedral framework cations (T = Al, Ti, P, Ga, Ge, and B). Typical examples of zeo-type materials are the microporous aluminophosphates (AlPOs), silicoaluminophosphates (SAPOs), and metal-containing aluminophosphates (MeAPOs) [6-9]. The incorporation of heteroatoms in zeolite framework contributes to the diversification of zeolite properties and thus to their potential uses. Crystalline microporous materials with penta- or hexa-coordinated heteroatoms are also considered as zeo-types, although they do not fulfill all conditions of the strict definition for a zeolite.

A major drawback of conventional zeolites is that their native microporous channel system could cause severe diffusion limitations, thus suppressing their catalytic activity in the reactions involving bulky molecules. The two major avenues explored to decrease the impact of transport limitations are the addition of meso- and/or macro-porosity to the inherent microporosity and the reduction of the size of the crystals [10-25].

Zeolites possessing a secondary pore system of meso/macro-pores are usually denoted as hierarchical zeolites. These materials attracted considerable attention and consequently, different synthetic methods were developed. These approaches can be sub-divided into two major groups: (1) the use of sacrificial hard- or soft-templates [26-30], and (2) post-synthesis chemical etching leading to partial dissolution of zeolite framework [25, 31-37].

The nanosized zeolites are obtained by conventional hydrothermal synthesis [38-43]. However, the synthesis, i.e., the composition of the initial system,

temperature - time conditions, are modified to facilitate the nucleation over the growth and hence to reduce the size of the crystals [12, 39, 44-45]. A nanosized zeolite is essentially a result of precise engineering of synthesis protocol in order to face a very demanding application. The decrease of the crystal size changes the ratio between the fraction of atoms exposed to the crystal surface and zeolite channels, which has a straightforward effect on zeolite accessibility and activity. Furthermore, nanosized zeolite crystals have a reduced diffusion path length compared to conventional micron-sized zeolites.

First studies on the synthesis of nano-sized zeolite were published by B. Schoeman et al. [46]. These studies were extended and deepened by V. Valtchev and S. Mintova. A characteristic feature of the early studies on zeolites is the extensive use of organic-structure directing agents (OSDAs). Nowadays, the use of OSDAs is still indispensable for the synthesis of high silica zeolites and some zeo-type materials. However, during the last decade, numerous efforts were dedicated to the preparation of nanosized zeolites employing alkali metal cations solely as structure-directing agents. These efforts are justified by a number of drawbacks related to the use of organic templates. In general, the use of organic templates, which are namely amines, is not appreciated since these are often toxic compounds which are not environmentally benign. Besides, the organic templates are relatively expensive and increase the price of the ultimate product. Moreover, the use of an organic template requires an additional post-synthesis, which is the combustion of the template at high temperature, typically about 550°C. This energy-intensive step is highly recommended to be omitted because of the negative impact on the environment, i.e., the emission of CO_2 and nitrogen-containing compounds. Hence, the preparation of nanozeolites using an alkali metal cation solely as a structure-directing agent offer significant advantages not only from economical but also from the environmental point of view. The synthesis of nanozeolites using only inorganic compounds could be considered to be a great extent as a green zeolite synthesis, which is the topic of the present paper. Figure 1 illustrates the economic and eco-environmental strategy of the

organic template-free fabrication of nanozeolites.

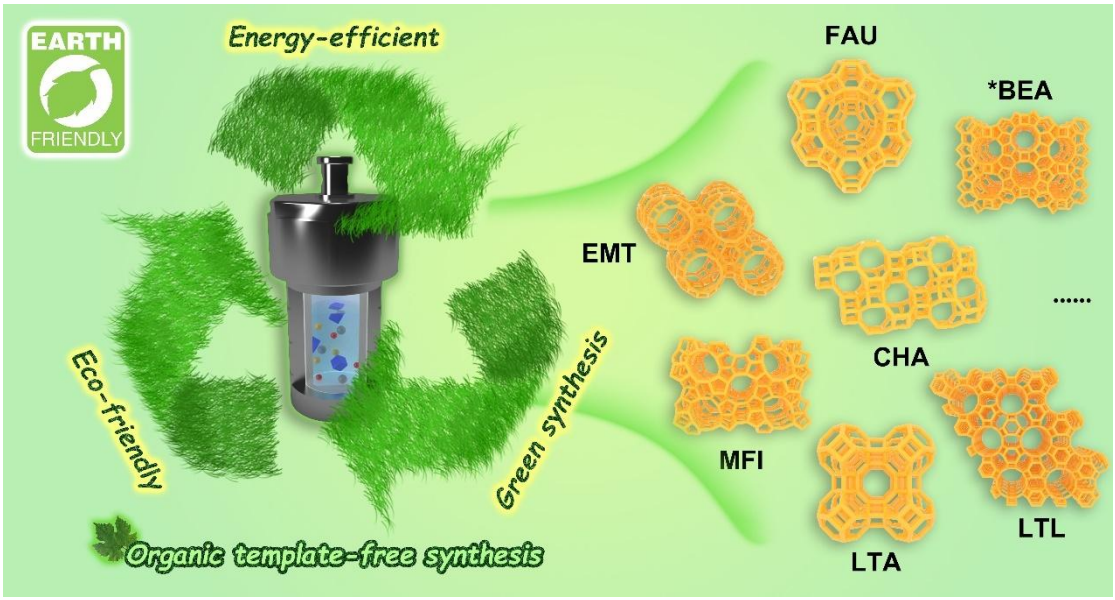

Figure 1. A green approach to the synthesis of nanozeolites.

This mini-review presents recent developments in the organic template-free synthesis of nanosized zeolites and related zeo-type molecular sieves. The strategies available for their preparation are discussed. The impact of the synthesis conditions on the physicochemical properties is also highlighted. Finally, the advantages and challenges of organic template-free synthesis of nanozeolites are addressed with particular attention to their potential applications.

2. Zeolite synthesis – a general introduction

Microporous zeo-type molecular sieves are synthesized under low-temperature hydrothermal conditions. The syntheses are performed under autogenous pressure, which rarely exceeds 10 bars. The first zeolite syntheses mimic the conditions in nature and namely, the zeolite formation in pegmatite veins, where the temperature of hydrothermal can reach more than 400°C [47-49]. Later, Milton [50] and Breck [51]

found out that using highly reactive alkaline aluminosilicate hydrogels allows a reduction of the synthesis time and synthesis temperature below 100°C, which opens the route to ambient pressure synthesis of zeolites.

Zeolites are typically synthesized under low temperature (room temperature to 170 ºC) hydrothermal/solvothermal conditions. The initial synthesis system is generally an aluminosilicate hydrogel that evolves under the coaction of mineralizing (OH^-, F^-) and structure-directing agents (SDAs). The SDAs could be organic molecules or alkali metal cations. Promoted by the Van Der Waals interactions, arranging SiO_4^- and AlO_4^- tetrahedra around the positively charged templating agent, such as organic molecules or hydrated alkali metal cations, is a generally accepted zeolite formation mechanism. Alkali metal ions are identified to be crucial for the synthesis of aluminosilicate zeolites. They boost Al incorporation into the framework. However, the obtained zeolite has to be ion-exchanged and the alkali metal is replaced with proton before use as a solid acid catalyst. Therefore, synthesis without alkali metal cations would be highly desirable as it would bring the synthesis process more facile, thus more economical and industrially effective. Especially, the conventional synthetic approaches for preparing nanozeolites are based on the extensive applications of organic templates [52]. The advantages of the organic template-assisted synthesis of nanozeolites are the effective control of the particle size. A great merit of the use of OSDAs is the possibility to stabilize a precursor zeolite suspension of high uniformity. The nucleation events in such a precursor are uniformly distributed in the system. Thus the formation of zeolite nuclei and their growth is uniform as well, which is indispensable for the formation of discrete zeolite nanocrystals with narrow particle size distribution. The stabilization of zeolite suspension using only alkali metal is difficult because of their strong surface charge and the aggregation of the silica particles, thus breaking the uniformity of the initial system. However, the utilization of organic templates brings serious disadvantages: (1) The organic templates are usually quaternary ammonium or amines, which are not eco-friendly. (2) Removal of organic templates generally requires high-temperature calcination to obtain the open

pores characteristic of molecular sieves. The calcination step is generally together with the release of hazardous gases (NO_x) and greenhouse gases (CO_2). The energy released by the combustion of the template combined with the generated water vapors can partially destroy the zeolite framework. (3) Most organic templates are expensive, and the calcination step for removing the organic agent increases the production cost. An alternative route to avoid the drawbacks of organic templates is to synthesize in the absence of them.

In general, a zeolite synthesis is performed in a batch reactor, where the growth stops with exhausting of the nutrient pool. Under such synthesis conditions, the ultimate crystal size can be adjusted by controlling the nucleation rate in the system. Increasing the number of nuclei generally results in a reduction in the final crystallite size. Therefore, the formation of small zeolite crystals requires conditions that are to nucleation rather than crystal growth. Hence, the guidance of the zeolite size requires precise control of the zeolite nucleation and the coinstantaneous crystal growth processes.

Significant effort has been focused on the development of organic template-free strategies to nanozeolites. Fine adjustment of the molar ratios of the starting gels is of particular importance in the synthesis of nanozeolites [41, 43]. Other approaches, including the utilization of zeolite seeds [53-57], space-confining agent [58-59] into the starting gels, and employing non-conventional heating mode (microwave-assisted, ultrasonic-assisted) [60-61] are also employed. The green route without using an organic template is very important for the preparation of zeolites, especially in large-scale industrial production. In the following section, the representative organic template-free strategies to nano zeolites are presented.

3. Organic template-free methods applied in the preparation of nanosized molecular sieves

The synthesis of nanozeolites using alkali metal cations solely is challenging due to

their strong positive charge, which generates inhomogeneities in the system. Consequently, the nucleation events are not simultaneous, which results in crystals of different sizes. Another negative impact of the alkali cations is that the crystallites are heavy agglomerated. In such systems, a very pronounced Ostwald ripening, which accentuates the differences in the crystal size, is often observed. Upon the Ostwald effect, the larger particles continue growing at the expense of the smaller ones, introduce additional heterogeneity in the system in terms of particle size.

3.1 Aluminosilicate zeolites

LTA-type

LTA-type zeolite is widely employed in ion-exchange and humidity-control applications. The abundant nucleation is a critical factor in the quest of nanosized zeolites, which control includes many parameters, as stated above. Low-temperature conditions mostly favor zeolite nucleation and lead to smaller crystal particles. Thus many attempts to decrease zeolite synthesis temperature below 100°C, and even below 80 °C were reported. Zeolite A is probably the best example of a low-temperature synthesis of a nanozeolite since it was successfully obtained at room temperature [62]. A drawback of low-temperature synthesis of zeolites is the long synthesis time. In the case of zeolite A, the optimization of synthesis parameters, such as the composition of the starting gel and the choice of reactants, allowed it's synthesis within 3 days. This is a reasonable period of time, which is not much longer than the conventional crystallization of low silica zeolites. After 3 days of room temperature crystallization, the crystal size of zeolite A ranged from 100 to 300 nm without well-developed crystal faces (Figure 2A). The prolongation of the synthesis time up to 10 days resulted in the formation of larger well-faceted cubic crystals in the range of 400 – 500 nm. Low-temperature synthesis of nanosized zeolite A was further studied by Dimitrov et al. [63]. The syntheses were performed at 35, 50, and 65 °C in the absence of OSDA. It was found that the crystal size of zeolite is a function of the crystallization temperature, as shown in Figure 2(B). The average crystal size was 30

– 100, 200, and 300 – 400 nm, respectively.

Another synthetic approach targeting nanozeolites is the vapor phase transport synthesis. This approach includes the use of an ultradense hydrogel offering a confined space, which is exposed to a water vapor atmosphere. This way, relatively large (~700 nm) zeolite A particles were obtained [63]. Confined synthesis of nanozeolites using a physical barrier limiting the growth was also reported. Zeolite A nanocrystals were synthesized under organic template-free hydrogel system by using *in-situ* thermoreversible polymer hydrogels [58]. The general synthesis scheme is illustrated in Figure 2(C). It was found that the size of the zeolites can be effectively controlled by a polymerized hydrogel. The zeolite A nanocrystals (40 – 80 nm) were prepared by using microwave-assisted heating in reverse microemulsion (water in oil) without using organic templates. The reverse microemulsion played a role as a space-confining nanoreactor (Figure 3(D)), while the microwave provided fast, uniform, and preferential heating of the aqueous phase where the zeolite crystals grew [59]. Microreactors are widely applied in the synthesis of organic and inorganic compounds. The most important advantages of microreactors are the fast transfer of mass and heat, excellent reaction kinetics, and high safety [64-65]. Zeolite A nanocrystals (100-240 nm) with well-developed crystal faces and uniform particle size distribution were synthesized using a manipulated organic template-free synthesis solution at 80 °C for 7.5 min in a two-phase liquid segmented microfluidic reactor [66]. The scheme of a two-phase liquid segmented microfluidic reactor employed in the synthesis of zeolite A nanocrystals is shown in Figure 2(E). Bead-milling was utilized in the treatment of organic template-free synthetic zeolites. By a combination of bead-milling and post-milling recrystallization, nano-zeolite A (~50 nm) with high crystallinity was successfully prepared in the absence of an organic template [67]. The synthetic process of nano-zeolite by bead-milling and post-milling recrystallization is illustrated in Figure 2(F). The yield of zeolite nanocrystals obtained by this method is almost 100%, since the preparation of nanozeolites by bead-milling and

recrystallization treatment does not cause material loss.

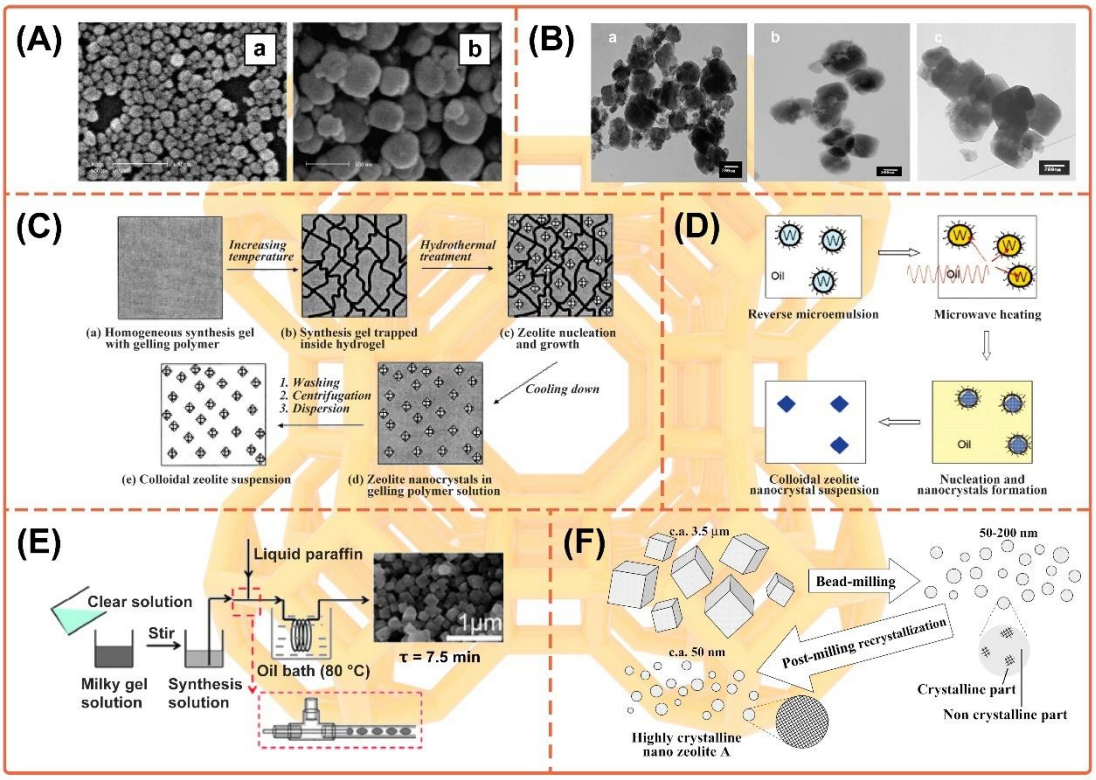

Figure 2. (A) SEM images of the zeolite A nanocrystals prepared at room temperature for 3 days (a) and 10 days (b). Reprinted with permission from ref. [62] (Copyright 2005, American Chemical Society). (B) TEM images of fully crystalline LTA-type materials obtained at 35 (a), 50 (b), and 65 ºC (c). Scale bar = 200 nm. Reprinted with permission from ref. [63] (Copyright 2011, American Chemical Society). (C) Schematic representation of the synthesis of template-free zeolite A nanocrystals by using in situ thermoreversible polymer hydrogels. Reprinted from ref. [58] (Copyright 2003, American Chemical Society). (D) Schematic representation of microemulsion-microwave synthetic method. Reprinted with permission from ref. [59] (Copyright 2005, American Chemical Society). (E) Scheme of synthesis of organic template-free zeolite A nanocrystals by employing a two-phase liquid segmented microfluidic reactor. Reprinted with permission from ref. [66] (Copyright 2009, Royal Society of Chemistry). (F) Scheme illustrating the construction process of nano-zeolite by bead milling and post-milling recrystallization. Reprinted with permission from ref. [67] (Copyright 2011, American Chemical Society).

EMT-type

An EMT-type framework possessing a 3D 12-member ring pore system is one of the most open zeolite structures [68]. EMT type zeolite is usually synthesized with the expensive 18-crown-6 as a template [69]. Due to the high cost, this material with great potential in the catalysis and separation processes has not been practically applied

[70-71]. Therefore, organic template-free synthesis of EMT-type nanosized zeolite is highly appealing. Ultrasmall EMT-type material was obtained by an organic template-free approach, as shown in Figure 3 [41]. The ultrasmall (6 – 15 nm) and nanosized (50 – 70 nm) EMT type materials were obtained under nearly ambient temperature conditions for 36 hours under conventional heating or for 4 min under microwave irradiation, respectively. Ng et al. pointed out that under such conditions, the crystal growth kinetics was slowed down, and the crystallization temperature influenced the size of EMT zeolites. Besides the small size, another great achievement is the narrow particle size distribution in the sodium-rich system, which makes the synthesis unique. In addition, Ng et al. also develop an organic template free method by using biomass rice husk ashes as a silica source to prepare nanosized EMT-type zeolite crystals with a diameter of 15 nm. The crystallization of EMT-type zeolite was completed within 28 h at 28 °C [72]. In 2019, Xiao's group reported a sustainable and efficient synthesis of nanosized EMT zeolite under organic template-free and solvent-free systems [73]. This approach not only completely avoids the utilization of an organic template but also effectively reduces the water pollution during the post-synthesis treatment. In comparison with conventional hydrothermal synthesis, the yield of EMT zeolites was substantially increased by this approach.

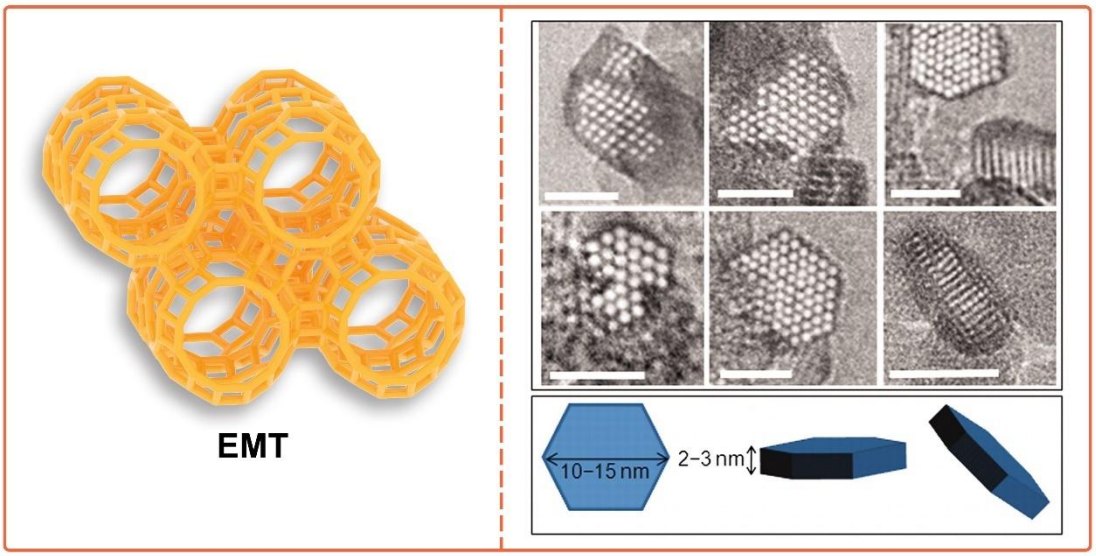

Figure 3. Ultrasmall EMT crystals with hexagonal morphology synthesized from template-free precursor suspension at 30°C for 36 hours. The individual crystals are with a size of 10 to 15 nm and a thickness of 2 to 3 nm. Scale bars represent 10 nm.

Reprinted with permission from ref. [41] (Copyright 2012, American Association for the Advancement of Science).

FAU-type

The importance of FAU-type zeolite for the petrochemical industry, particularly in the fluid catalytic cracking (FCC) process, has attracted worldwide research interest to its synthesis in a nanosized form. In 2014, the feasibility of FAU-type nanocrystals synthesis from an organic template-free condition was first reported by Valtchev and Bozhilov [74]. The study focused on the formation mechanism of FAU-type X zeolite that was prepared at ambient temperature for three weeks. The particle size of the individual crystal was below 30 nm, building spherical aggregates of 150 – 200 nm in size. The synthesis of even smaller crystals (10 – 20 nm) was also reported. The extension of aging time increased the size of the crystallites; however, the size of the aggregate remains unchanged (Figure 4). Based on the similar gel system, Huang et al. prepared nanosized zeolite Y crystals via a three-stage synthesis procedure [75]. Specifically, the synthesis gel was firstly aged at room temperature for 24 h, then was heated to 38 °C and kept for 24 h prior to hydrothermally treating at 60 °C for 48 h. Hierarchical porous aggregated particles (190 and 600 nm) composed from well-crystallized zeolite NaY nanocrystals were obtained without adding any organic template. Awala et al. developed the rational design for the template-free synthesis of nanosized FAU zeolites [42]. The obtained nanosized FAU zeolites possessed ultra-small crystallites with a narrow particle size distribution (10 – 15 nm), and high crystalline yield (above 80%). The micropore volume (0.30 cm^3 g^{-1}) of the nano Y was typical of highly crystalline FAU-type materials. Again by regulating the synthesis temperature, the particle size was controlled from 10 nm to 70 nm keeping the particle size distribution very narrow. In comparison with the conventional micrometer-sized counterparts, the Si/Al ratios of the obtained materials could be adjusted between 1.1 and 2.1 (zeolites X or Y), and showed superior thermal stability thereby giving excellent catalytic activity in the dealkylation of a bulky molecule, such as 1,3,5-triisopropylbenzene. This result demonstrates high accessibility of the

active sites in nanozeolites, in particular those with size below 50 nm.

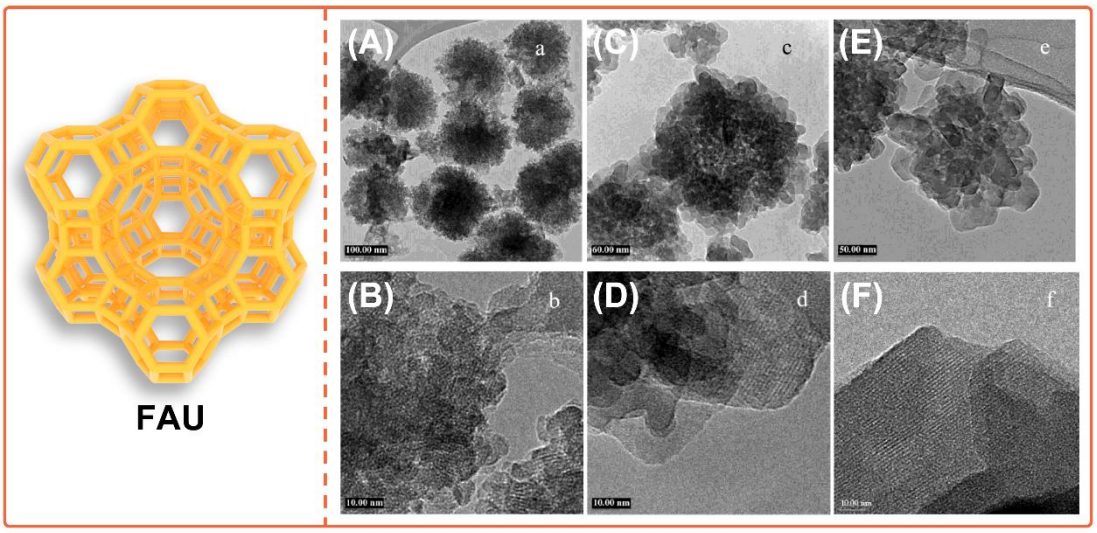

Figure 4. Low and high magnification TEM micrographs of the crystals obtained after 17 days (A, B), 22 days (C, D), and 38 days (E, F) ageing. Reprinted with permission from ref. [74] (Copyright 2004, American Chemical Society).

MFI-type

MFI-type zeolites are a significant industrial catalyst and separation material [76]. Conventionally ZSM-5 (MFI-type) is synthesized with tetrapropylammonium as a template. Recently the works on nanosized MFI-type zeolites focusing on economic and eco-friendly syntheses were reported [77-78]. The preparation of ZSM-5 nanocrystals by using seeds-assisted crystallization from an organic template-free gel system was published by Majano et al. [77]. ZSM-5 nanozeolite crystals were synthesized using a gel system containing 0.1, 1.0, and 3.0 wt % of 80 nm silicalite-1 seeds for SiO_2 content in the synthesis gel. The size of resulting ZSM-5 particles (mainly aggregates) ranged from 140 to 230 nm. The seed content strongly influenced the size of the obtained crystal. Another advantage of this approach is the high yield, which is above 80%. However, a disadvantage of this method is the high aggregation of the crystals compared with the syntheses using clear sols rich in tetrapropylammonium hydroxides.

Other zeolites

The list of nanosized aluminosilicate zeolites obtained from organic template-free systems is longer. For instance, important zeolites as L [79-80], Beta [81], Mordenite [82], and others were successfully synthesized in nanosized form using some of the above approaches. The initial system employed and the synthesis conditions used for these syntheses are summarized in Table 1. The one-dimensional pore system of zeolite L was found appropriate for optical applications and crystallites with different sizes, including nanosized, were synthesized and further modified to fit to this application [83-84]. Garcia-Martinez and Rimer and their co-workers reported the preparation of ultrasmall (ca. 30 nm) zeolite L crystals with uniform size by employing an organic template-free method [80]. The homogeneous distribution of K^+ ions throughout the silicate precursor is related to the enhanced nucleation rate, and thus the formation of ultrasmall LTL-type nanocrystals. Zeolite Beta with 12-ring three-dimensional pore system is widely used in several important commercial processes. Zhou et al. reported a one-pot organic template-free synthesis of single-crystalline nanosized hierarchical zeolite beta with 200 – 300 nm. This result was achieved by introducing sodium carbonate in the precursor solution [81]. The obtained material featured abundant and interconnected mesopores crossing the entire crystal. The obtained zeolite Beta exhibits a high BET surface area (667 m^2 g^{-1}) and a high total pore volume (0.65 cm^3 g^{-1}) that is due to mesopores centered at 2 – 8 and 90 – 150 nm. The one-pot sodium carbonate-assisted approach had also been successfully applied to other zeolites. The mordenite is an important catalyst utilized in petroleum refining. Zhang et al. proposed nano-Beta seeds and organic template-free aluminosilicate gel can be converted to mordenite with nanosized dimensions [82]. Thus obtained MOR-type zeolite possessed abundant inter-crystallite mesopores and high crystallinity (Figure 5). TEM images showed that the particles are composed of abundant mordenite nanocrystals with an average diameter of ca. 20 nm. The above studies explicitly demonstrate the possibility of synthesizing zeolite nanocrystals from organic template-free systems with high crystallinity and yield, and often a narrow particle size distribution.

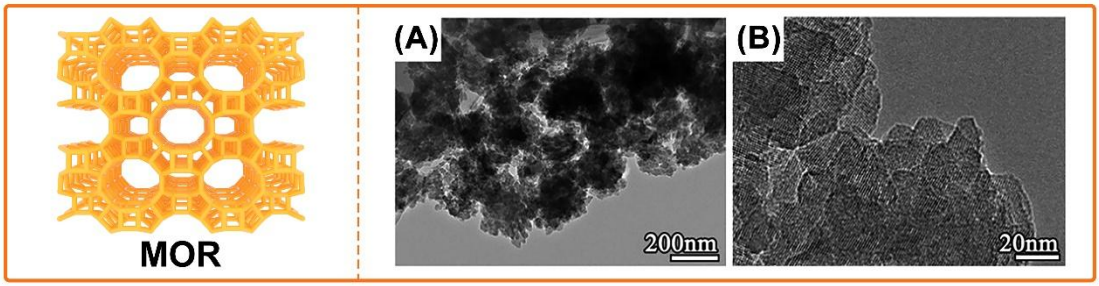

Figure 5. (A) Low and (B) high magnification TEM images of mordenite nanocrystals. Reprinted with permission from ref. [82] (Copyright 2016, The Royal Society of Chemistry.).

Table 1. Synthesis conditions and crystal size of the aluminosilicate nanozeolites synthesized from organic template-free systems.

Framework type	Molar composition of the clear synthesis solution (S) or gel (G)	Temp, °C	Si/Al	Crystal size range, nm	Ref.
LTA	$3.56Na_2O$: $1.59SiO_2$: $1.00Al_2O_3$: $32.12H_2O$: 3.48MC (S)	80	-	70	[58]
LTA	$3.67Na_2O$: $1.65SiO_2$: $1Al_2O_3$: $83.93H_2O$: 7.08MC (S)	80	-	98	[58]
LTA	$5.85Na_2O$: $2.7SiO_2$: $1.00Al_2O_3$: $182H_2O$: 36.4CTAB: 364*n*-butanol: 4732cyclohexane (G)	75	-	40-80	[59]
LTA	3-8Na_2O: 0.4-0.55Al_2O_3: 1.0SiO_2: 80-150H_2O (G)	25 ± 1	-	100-300	[62]
LTA	3-8Na_2O: 0.4-0.55Al_2O_3: 1.0SiO_2: 80-150H_2O (G)	25 ± 1	-	400-500	[62]
LTA	20mL MGS [a] + 10 mL SCS [b](G)	80	1.3	60-260	[66]
LTA	20mL MGS [a] + 10 mL SACS [c] (G)	80	1.1	80-260	[66]
LTA	20mL MGS [a] + 10 mL ACS [d] (G)	80	0.7	80-360	[66]
LTA	20mL MGS [a] + 5 mL SACS [c] (G)	80	1.0	80-275	[66]
LTA	20mL MGS [a] (G)	80	0.8	80-320	[66]
LTA	20mL MGS [a] + 10 mL SACS [c] (G)	80	1.1	95-230	[66]
LTA	20mL MGS [a] + 10 mL SACS [c] (G)	80	1.1	60-430	[66]
LTA	$6Na_2O$: $0.505Al_2O_3$: $1.0SiO_2$: $150H_2O$(G)	50	-	200	[63]
LTA	$6Na_2O$: $0.505Al_2O_3$: $1.0SiO_2$: $150H_2O$(G)	65	-	300-400	[63]

Table 1 Continued.

Framework type	Molar composition of the clear synthesis solution (S) or gel (G)	Temp, °C	Si/Al	Crystal size range, nm	Ref.
LTA	$405Na_2O$: $1Al_2O_3$: $51SiO_2$: $29900H_2O$ (S)	90	<20.0	50	[67]
EMT	$5.15SiO_2$: $1Al_2O_3$: $18.45Na_2O$: $240.3H_2O$ (G)	30	1.1	6-15	[41]
EMT	$5SiO_2$: $1Al_2O_3$: $17.48Na_2O$: $340.3H_2O$ (G)	30	-	50-70	[41]
EMT	$18.45Na_2O$: $5.15SiO_2$: $1Al_2O_3$: $240.3H_2O$ (S)	30	1.1	8-18	[79]
EMT	$5SiO_2$: $1Al_2O_3$: $18Na_2O$: $217H_2O$ (G)	28	1.3	15	[72]
EMT	$16NaAlO_2$: $0.5Na_2SiO_3 \cdot 9H_2O$: $1.3SiO_2 \cdot 1.67H_2O$ (G)	110	1.2	30-150	[73]
FAU	$4Na_2O$: $0.2Al_2O_3$: $1.0SiO_2$: $200H_2O$(G)	25 ± 1	1.2	10-20	[74]
FAU	$9.6Na_2O$: $1.0Al_2O_3$: $14.4SiO_2$: 175.3, 198.0, 220.7, 243.4, 288.8, $334.2H_2O$ (G)	60	1.5-1.8	160-700	[75]
FAU	$9Na_2O$: $0.7Al_2O_3$: $10SiO_2$: $160H_2O$ (G)	50	1.6	10	[42]
FAU	$8Na_2O$: $0.7Al_2O_3$: $10SiO_2$: $160H_2O$ (G)	120	1.7	70	[42]
FAU	$8Na_2O$: $1Al_2O_3$: $10SiO_2$: $400H_2O$ (G)	100	2.1	400	[42]
MFI	$7.4Na_2O$: $0.88Al_2O_3$: $25SiO_2$: $1168H_2O$ + 3 wt% seeds (S)	100	10.2	30-70	[77]
MFI	$7.4Na_2O$: $0.88Al_2O_3$: $25SiO_2$: $1168H_2O$ + 3 wt% seeds (S)	120	10.1	30-70	[77]
MFI	$7.4Na_2O$: $0.88Al_2O_3$: $25SiO_2$: $1168H_2O$ + 3 wt% seeds (S)	150	9.6	130-160	[77]
MFI	$7.4Na_2O$: $0.88Al_2O_3$: $25SiO_2$: $1168H_2O$ + 3 wt% seeds (S)	170	10.0	>200,400-700	[77]

Table 1 Continued.

Framework type	Molar composition of the clear synthesis solution (S) or gel (G)	Temp, °C	Si/Al	Crystal size range, nm	Ref.
MFI	$1SiO_2$: $0.033Al_2O_3$: $0.1Na_2O$: $24H_2O$ + 0.015seeds (G)	175	14.2	600-800	[78]
LTL	$5K_2O$: $10SiO_2$: $0.5Al_2O_3$: $200H_2O$ (S)	170	2.6	8-18	[79]
LTL	0.5 Al_2O_3: 20 SiO_2: $10.2K_2O$: $1030H_2O$ (S)	180	20	<30	[80]
LTL	0.5 Al_2O_3: $36.7SiO_2$: $10.2K_2O$: $1030H_2O$ (S)	180	35	<30	[80]
BEA	$1Na_2CO_3$: Al_2O_3: $50SiO_2$: 15TEAOH: $500H_2O$ (S)	150	29.0	200-300	[81]
MOR	$10SiO_2$: $0.25Al_2O_3$: $3.25Na_2O$: 4.5NaF: 160-$270H_2O$ + 7.0 wt% seeds (G)	160	9.7	<150	[82]
ANA	$16.5SiO_2$: $1Al_2O_3$: $5.3Cs_2O$: $175H_2O$ (S)	180	4.1	79.4	[85]
ABW	$4SiO_2$: $1Al_2O_3$: $16Cs_2O$: $164H_2O$ (S)	180	1.08	68	[60]
CAN	$4.0Na_2O$: $1.0Al_2O_3$: $4.0SiO_2$: $32.6H_2O$ (S)	120	~1.2	200-800	[86]
EDI	$4SiO_2$: $1Al_2O_3$: $16K_2O$: $160H_2O$ (G)	100	1.19	27,300	[87]
LTJ	$3.75SiO_2$: $1Al_2O_3$: $15K_2O$: $132H_2O$ (G)	100	1.86	220	[88]
MER	$0.5SiO_2$: 1KOH: $8H_2O$: $0.026Al_2O_3$ (S)	170	-	50	[89]
MER	$0.5SiO_2$: 1KOH: $20H_2O$: $0.026Al_2O_3$ (Precipitate)	170	-	10	[89]

Table 1 Continued.

Framework type	Molar composition of the clear synthesis solution (S) or gel (G)	Temp, °C	Si/Al	Crystal size range, nm	Ref.
MER	$1Al_2O_3$: $7SiO_2$: $3.5K_2O$: $196H_2O$ (S)	180	2.28	140	[90]
RHO	$10SiO_2$: $0.8Al_2O_3$: $8Na_2O$: $0.58Cs_2O$: $100H_2O$ (S)	90	1.5	<100	[91]
SOD	$1.0Al_2O_3$: $3.8SiO_2$: $2.1Na_2O$: $50H_2O$ (G)	100	-	60-80	[92]

- not shown

[a] MGS: $6.5Na_2O$: $0.6Al_2O_3$: $1.0SiO_2$: $150H_2O$, [b] SCS: $8.6Na_2O$: $1.0SiO_2$: $150H_2O$ [c] SACS: $8.6Na_2O$: $0.18Al_2O_3$: $1.0SiO_2$: $150H_2O$, [d] ACS: $8.6Na_2O$: $0.18Al_2O_3$: $150H_2O$

3.2 AlPO and SAPO materials

In 1982, Wilson *et al.* reported a new class of crystalline, microporous materials, which represented the first family of framework oxide molecular sieves synthesized without silica [93]. These aluminophosphates (AlPO), similarly to zeolites, are synthesized under low-temperature hydrothermal conditions using organic amine as SDAs. As discussed in the introduction section, the elimination of the organic template requires high-temperature combustion with all undesired economic and environmental consequences. Thus, the quest for more green syntheses desires an extensive decrease or avoidance of the utilization of organic amine.

Ionic liquids have aroused great attention in many fields as a synthesis medium, especially for the replacement of organic solvents, which represent a green alternative of the conventional synthesis [94-95]. A nanosized manganese-containing aluminophosphate MnAlPO-5 (AFI-type) was prepared using this approach. This material was synthesized by ionothermal synthesis in the presence of 1-ethyl-2,3-dimethylimidazolium bromide under ambient conditions [96]. The ionic liquid was employed as both a solvent and a template. The size of the resulting particles was 80 nm. NKX-2 is an important intermediate for the synthesis of useful microporous aluminophosphates, such as SAPO-46, SAPO-31, AlPO-11, AlPO-5 and AlPO-CJ2, etc.. Aluminophosphite NKX-2 with rod-like morphology and a high c/a axis aspect ratio (~10) was ionothermally synthesized using 1-ethyl-2,3-dimethylimidazolium bromide (EMMIMBr) ionic liquid [97]. Noteworthy, the synthesis completed in an open vessel for about 3 h.

In 2016, via an organic template-free route, the NaNKX-2 aluminophosphite was prepared [98]. This non-conventional synthesis involves H_3PO_3 as a phosphorous source and NaOH as an inorganic base and template. In 2020, an open-framework SAPO material with a composition of $Cs_2(Al_{0.875}Si_{0.125})_4(P_{0.875}Si_{0.125}O_4)_4(HPO_4)$ was synthesized by Fan et al. in an organic template-free caesium-containing system under hydrothermal conditions [99]. The replacement of the organic template by inorganic Cs^+ ions makes the current synthesis protocol eco-friendly. Notably, the incorporated Cs^+ endowed the material with improved thermal stability and high proton/ionic conductivity. However, it is clear that this approach cannot be applied to the synthesis of all AlPO- and SAPO-type materials.

3.3 Other zeo-type molecular sieves

Microporous manganese oxide octahedral molecular sieves (OMS) are essential materials in

environmental chemistry, electrochemistry, and heterogeneous catalysis [100]. Structurally these materials are not zeolites since their framework is built of octahedral manganese units. On the other side, they are crystalline microporous materials with properties similar to zeolites, which justifies their inclusion in the present review. The structure and morphology of several OMS materials are shown in Figure 6. Most of the structures exhibit long prismatic morphology with a thickness of 50 to 100 nm. There is also a plate-like material as gama-MnO_2 with a size of about 200 nm.

An important feature of the OMS materials synthesis is that no organic template is involved. Thus the synthesized material does not require high-temperature calcination. Shen et al. first prepared OMS-1 material by reactions of MnO_4^- and Mn^{2+} under alkaline conditions [101]. OMS-1 possessed a thermally stable 3 × 3 tunnel structure, the mixed-valent semiconducting nature, excellent adsorptive properties, and remarkable activity in numerous catalytic reactions. Another OMS phase that shows interesting electrochemical and catalytic properties is the OMS-2 structure type with 4.6 Å square pores [102]. Yuan et al. reported the synthesis of mesoporous hollow nanospheres of OMS-2 type built up of nanosized particles [103]. These nanospheres with hexagonal flake shape and a size of approximately 400 nm in diameter showed excellent activity in oxidation reactions due to enhanced surface area. Later, Shen et al. developed a variety of OMS materials with different pore sizes and tunnel structures using the Na^+ cation as a structure-directing agent. These reports clearly demonstrated that similarly to zeolites, the synthesis of OMS materials can be controlled to a great extent using alkali metal cations solely [104]. The conventional routes for preparing OMS-2 include hydrothermal treatment using a sol-gel approach with reaction time varying from hours to days. De Guzman et al. prepared OMS-2 by using refluxing under a redox reaction in 24 h [105]. Yuan et al. synthesized OMS-2 material within 12 h by employing $K_2Cr_2O_7$ and $MnSO_4$ [106]. Morphologies of OMS-2 nanoparticles can be tuned by varying reaction temperatures. At low temperature (120 °C), OMS-2 exhibited dendritic nanoclusters, while at high temperature (180 °C) spherical dandelion-like microspheres are obtained. Via the utilization of $K_2S_2O_8$ and $MnSO_4$, Yuan et al. also synthesized OMS-2 nanowires in a 3 days hydrothermal synthesis [107]. Microwave-assisted synthesis has also been used to prepare OMS-2 materials [108]. Through the assistance of microwaves in the hydrothermal condition, the preparation of OMS-2 can be achieved in 10 s. The formation of crystalline phase OMS-2 material occurred when the reaction temperature is higher than 100 ºC, whereas reaction temperatures below 80 ºC led to an amorphous manganese oxide material. The OMS-2 thin

nanoflakes convert to nanowires with increased reaction temperature. However, this microwave-assisted hydrothermal approach still requires high temperatures (above 150 °C) and at least 2 bar pressure. The utilization of ultrasound in the synthesis of the OMS nanomaterials significantly reduced reaction times and temperatures. For instance, Dharmarathna et al. developed the ultrasonic-assisted synthesis of OMS-2 materials possessing a high specific surface area of 288 ± 1 m^2/g [109]. In comparison with reflux methods (88 ± 1 m^2/g), the specific surface area increased three times, while reaction time decreased by 50% under cosolvent systems.

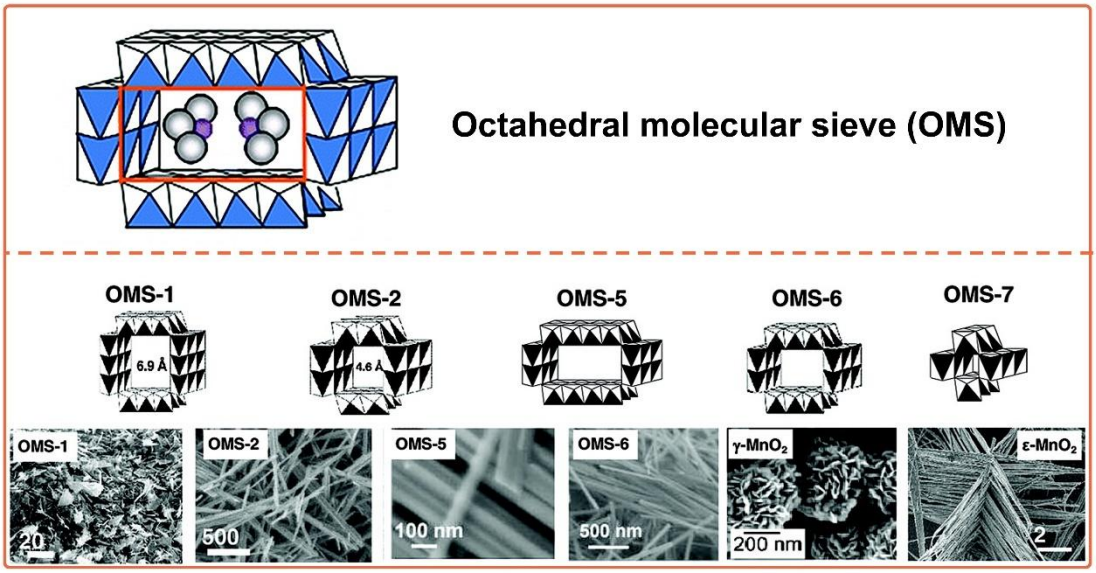

Figure 6. Structures and morphologies for various OMS materials. Reprinted with permission from ref. [100] (Copyright 2008, American Chemical Society).

4. Applications

Zeolite nanocrystals synthesized under organic templates-free conditions offer great potential for uses in heterogeneous catalysis, adsorption, and separation processes. Besides, the recent developments show that nanosized molecular sieves are in the focus of emerging nanotechnology applications, including sensors, medicine, biological and pharmaceutical industries [110]. There are substantial differences when nano-sized and conventional (micron-sized) zeolite crystals are used for catalytic reactions. The nanocrystals featuring large external surface areas are beneficial for the conversion of bulky molecules that cannot penetrate in zeolite channels. In addition, the nanocrystals offer the advantage of a shorter diffusion path, thus minimizing the effect of undesired side reactions [12]. The impact of the external surface of FAU-type nanocrystals in the dealkylation of a bulky molecule, 1,3,5-triisopropylbenzene

was studied compared with a conventional micron-sized industrial sample [42]. All obtained nanosized zeolite catalysts showed higher catalytic activity with respect to the high-quality commercial sample. The product selectivity at 200 °C provided further insight into their superior catalytic performance. The excellent colloidal stability of nanosized zeolites is also useful for their uniform dispersion on supports and the preparation of thin-to-thick coatings [111-112]. Flexible nanosized RHO-type zeolite containing only inorganic cations (Na^+ and Cs^+) has been synthesized under an organic template-free system at 90 °C for 1 h [91]. Due to the high Cs content, the thermal stability of the RHO nanocrystals showed improved thermal stability. The flexible RHO-type nanosized zeolite showed excellent selectivity toward CO_2 over CH_4 attributed to the ability of the Cs^+ cation to displace out from and into the D8R window.

Different types of zeolite nanocrystals, for instance, EMT, LTA, LTL, MFI, MOR, FAU, have different sizes, compositions and shapes, their cytotoxic activity is low[110]. Thus these materials are safe for using in biological and medical applications. More specialized studies were performed on EMT- and LTL-type zeolites synthesized without organic template that proved to be non-toxic to HeLa cells [110]. EMT- and FAU-type nanoparticles showed specific adsorption abilities for human plasma proteins.[113] These two zeolites exposed to high plasma concentration (100%) exhibited highly selective adsorption for polipoprotein C-III (APOC-III) and fibrinogen. At low plasma concentration (10 %), high selective adsorption for immunoglobulin gamma (i.e. IGHG1, IGHG2 and IGHG4) proteins was observed. This study revealed the potential of nanozeolites in the therapies of hemophilia B (F-IX deficient)) with a risk of bleeding and hemophilic patients (hemophilia A (F-VIII deficient). Nanozeolites also give promises in the preparation of selective chemical sensors for detection of exhaust gases, hydrocarbons and biomolecules [114].

5. Conclusion and outlook

Progresses in nanoscience are continually being implemented in industry and our everyday life, from advanced technologies to domestic products. The growing environmental and economic concerns continuously boost the development of microporous nanomaterials. The analysis of the literature reveals that crystalline molecular sieve nanocrystals can be easily synthesized and scaled up at low temperatures without the release of any harmful compounds. These nanoscale molecular sieves materials offer bright

futures for a great variety of technologies and commodity products. The possible green mass production of nanosized molecular sieves provides remarkable opportunities for applications in catalysis, adsorption, and separations involving larger molecules and for designing thin films, membranes, or emerging nanoscale devices.

The industrial implementation of nanozeolite-based technology will depend on future developments in the field. The most urgent issues to be addressed are: (1) the extension of Si/Al ratio in important zeolites as FAU-, LTA- and EMT-type; (2) the development of organic template-free synthesis of nanosized zeolites without aggregation and impurities; (3) the improved colloidal stability of nanosized molecular sieves; and (4) the synthesis of various of nanosized molecular sieve materials, such as AlPO, SAPO, MeAPO, without the use of an organic template agent.

This mini-review summarizes the significant issues related to the preparation of crystalline nanosized molecular sieves under the organic template-free condition. Addressing these issues will open the door to a more eco-friendly and economical design of high-performing materials and guide the future research direction in this field.

Acknowledgements

This work is supported by the National Natural Science Foundation of China (Grant 21971082 and 22001090) and the Jilin Province Science and Technology Development Plan (Grant 20190201229JC and 20200201096JC). And this work acknowledges 111 Project (B17020). X.C. and V.V. acknowledge the collaboration in the framework of joint Sino-French international laboratory “Zeolites”.

References

[1] M.E. Davis, Nature 417 (2002) 813-821.
[2] A. Corma, Chem. Rev. 95 (1995) 559-614.
[3] Z. Wang, J. Yu, R. Xu, Chem. Soc. Rev. 41 (2012) 1729-1741.
[4] X. Wei, Y. Wang, A.J. Hernández-Maldonado, Z. Chen, Green Energy & Environ. 2 (2017) 363-369.
[5] Y. Li, J. Yu, Chem. Rev. 114 (2014) 7268-7316.
[6] S. Mintova, S. Mo, T. Bein, Chem. Mater. 10 (1998) 4030-4036.
[7] J. Yu, R. Xu, Acc. Chem. Res. 36 (2003) 481-490.

[8] J. Yu, R. Xu, Chem. Soc. Rev. 35 (2006) 593-604.
[9] G. Li, B. Wang, Q. Sun, W.Q. Xu, Z. Ma, H. Wang, D. Zhang, J. Zhou, Green Energy & Environ. 4 (2019) 470-482.
[10] S. Mintova, J.-P. Gilson, V. Valtchev, Nanoscale 5 (2013) 6693-6703.
[11] S. Mintova, M. Jaber, V. Valtchev, Chem. Soc. Rev. 44 (2015) 7207-7233.
[12] V. Valtchev, L. Tosheva, Chem. Rev. 113 (2013) 6734-6760.
[13] S. Lopez-Orozco, A. Inayat, A. Schwab, T. Selvam, W. Schwieger, Adv. Mater. 23 (2011) 2602-2615.
[14] Y. Wei, T.E. Parmentier, K.P. De Jong, J. Zečević, Chem. Soc. Rev. 44 (2015) 7234-7261.
[15] D. Verboekend, N. Nuttens, R. Locus, J. Van Aelst, P. Verolme, J.C. Groen, J. Pérez-Ramírez, B.F. Sels, Chem. Soc. Rev. 45 (2016) 3331-3352.
[16] W. Schwieger, A.G. Machoke, T. Weissenberger, A. Inayat, T. Selvam, M. Klumpp, A. Inayat, Chem. Soc. Rev. 45 (2016) 3353-3376.
[17] V. Valtchev, S. Mintova, Mrs Bull 41 (2016) 689-693.
[18] J. Pérez-Ramírez, C.H. Christensen, K. Egeblad, C.H. Christensen, J.C. Groen, Chem. Soc. Rev. 37 (2008) 2530-2542.
[19] Q. Sun, Z. Xie, J. Yu, Natl. Sci. Rev. 5 (2018) 542-558.
[20] R. Bai, Y. Song, Y. Li, J. Yu, Trends Chem. 1 (2019) 601-611.
[21] L. Tosheva, V.P. Valtchev, Chem. Mater. 17 (2005) 2494-2513.
[22] G. Yang, J. Han, Y. Liu, Z. Qiu, X. Chen, Chin. J. Chem. Eng. (2020) https://doi.org/10.1016/j.cjche.2020.1006.1026.
[23] G. Yang, Y. Wei, S. Xu, J. Chen, J. Li, Z. Liu, J. Yu, R. Xu, J. Phys. Chem. C 117 (2013) 8214-8222.
[24] Evam. Gallego, C. Paris, M.R. Díaz-Rey, M.E. Martínez-Armero, J. Martínez-Triguero, C. Martínez, M. Moliner, A. Corma, Chem. Sci. 8 (2017) 8138-8149.
[25] G. Yang, J. Han, Y. Huang, X. Chen, V. Valtchev, Chin. J. Chem. Eng. 28 (2020) 2022-2027.
[26] I. Schmidt, A. Krogh, K. Wienberg, A. Carlsson, M. Brorson, C.J.H. Jacobsen, Chem. Commun. (2000) 2157-2158.
[27] I. Schmidt, A. Boisen, E. Gustavsson, K. Ståhl, S. Pehrson, S. Dahl, A. Carlsson, C.J.H. Jacobsen, Chem. Mater. 13 (2001) 4416-4418.
[28] Y. Tao, H. Kanoh, K. Kaneko, J. Am. Chem. Soc. 125 (2003) 6044-6045.
[29] M. Choi, K. Na, J. Kim, Y. Sakamoto, O. Terasaki, R. Ryoo, Nature 461 (2009) 828-828.
[30] A. Sachse, J. García-Martínez, Chem. Mater. 29 (2017) 3827-3853.
[31] X. Chen, A. Vicente, Z. Qin, V. Ruaux, J.-P. Gilson, V. Valtchev, Chem. Commun. 52 (2016) 3512-3515.
[32] X. Chen, D. Xi, Q. Sun, N. Wang, Z. Dai, D. Fan, V. Valtchev, J. Yu, Microporous Mesoporous Mater. 234 (2016) 401-408.
[33] Y. Pan, G. Chen, G. Yang, X. Chen, J. Yu, Inorg. Chem. Front. 6 (2019) 1299-1303.
[34] Z. Qin, J.-P. Gilson, V. Valtchev, Curr. Opin. Chem. Eng. 8 (2015) 1-6.
[35] Z. Qin, L. Hafiz, Y. Shen, S.V. Daele, P. Boullay, V. Ruaux, S. Mintova, J.-P. Gilson, V. Valtchev, J. Mater. Chem. A 8 (2020) 3621-3631.
[36] Z. Qin, L. Lakiss, J.-P. Gilson, K. Thomas, J. Goupil, C. Fernandez, V. Valtchev, Chem. Mater. 25 (2013) 2759-2766.
[37] G. Yang, Z. Qiu, J. Han, X. Chen, J. Yu, Mater. Chem. Front. (2020) https://doi.org/10.1039/D1030QM00388C.

[38]Q. Zhang, S. Xiang, Q. Zhang, B. Wang, A. Mayoral, W. Liu, Y. Wang, Y. Liu, J. Shi, G. Yang, J. Luo, X. Chen, O. Terasaki, J.-P. Gilson, J. Yu, Chem. Mater. 32 (2020) 751-758.
[39]Q. Zhang, A. Mayoral, O. Terasaki, Q. Zhang, B. Ma, C. Zhao, G. Yang, J. Yu, J. Am. Chem. Soc. 141 (2019) 3772-3776.
[40]Q. Zhang, G. Chen, Y. Wang, M. Chen, G. Guo, J. Shi, J. Luo, J. Yu, Chem. Mater. 30 (2018) 2750-2758.
[41]E.-P. Ng, D. Chateigner, T. Bein, V. Valtchev, S. Mintova, Science 335 (2012) 70.
[42]H. Awala, J.-P. Gilson, R. Retoux, P. Boullay, J.-M. Goupil, V. Valtchev, S. Mintova, Nat. Mater. 14 (2015) 447-451.
[43]E.-P. Ng, J.-M. Goupil, A. Vicente, C. Fernandez, R. Retoux, V. Valtchev, S. Mintova, Chem. Mater. 24 (2012) 4758-4765.
[44]S. Mintova, N.H. Olson, T. Bein, Angew. Chem. Int. Ed. 38 (1999) 3201-3204.
[45]L. Itani, K.N. Bozhilov, G. Clet, L. Delmotte, V. Valtchev, Chem. Eur. J. 17 (2011) 2199-2210.
[46]B.J. Schoeman, J. Sterte, J.-E. Otterstedt, J. Chem. Soc., Chem. Commun. (1993) 994-995.
[47]R.M. Barrer, J. Chem. Soc. (1948) 127–132.
[48]R.M. Barrer, J. Chem. Soc. (1948) 2158–2163.
[49]R.M. Barrer, Zeolites and Clay Minerals as Sorbents and Molecular
Sieves, Academic Press: London, 1978.
[50]R.M. Milton, ed. Robson, M. L. O. a. H. E., ACS Symp. Ser., 1989, p. P.1.
[51]D. Breck, Zeolite Molecular Sieves, John Wiley and Sons: New York, 1974.
[52]C.S. Cundy, P.A. Cox, Chem. Rev. 103 (2003) 663-702.
[53]B. Xie, H. Zhang, C. Yang, S. Liu, L. Ren, L. Zhang, X. Meng, B. Yilmaz, U. Müller, F.-S. Xiao, Chem. Commun. 47 (2011) 3945-3947.
[54]H. Zhang, C. Yang, L. Zhu, X. Meng, B. Yilmaz, U. Müller, M. Feyen, F.-S. Xiao, Microporous Mesoporous Mater. 155 (2012) 1-7.
[55]Y. Kamimura, W. Chaikittisilp, K. Itabashi, A. Shimojima, T. Okubo, Chem Asian J 5 (2010) 2182-2191.
[56]B. Xie, J. Song, L. Ren, Y. Ji, J. Li, F.-S. Xiao, Chem. Mater. 20 (2008) 4533-4535.
[57]Y. Kamimura, S. Tanahashi, K. Itabashi, A. Sugawara, T. Wakihara, A. Shimojima, T. Okubo, J. Phys. Chem. C 115 (2011) 744-750.
[58]H. Wang, B.A. Holmberg, Y. Yan, J. Am. Chem. Soc. 125 (2003) 9928-9929.
[59]Z. Chen, S. Li, Yan, Chem. Mater. 17 (2005) 2262-2266.
[60]T.M.A. Ghrear, Y.-W. Cheong, G.K. Lim, D. Chateigner, T.C. Ling, S.H. Tan, E.-P. Ng, Mater. Res. Bull. 122 (2020) 110691.
[61]R. Khoshbin, R. Karimzadeh, Adv Powder Technol 28 (2017) 973-982.
[62]V.P. Valtchev, L. Tosheva, K.N. Bozhilov, Langmuir 21 (2005) 10724-10729.
[63]L. Dimitrov, V. Valtchev, D. Nihtianova, Y. Kalvachev, Cryst. Growth Des. 11 (2011) 4958-4962.
[64]K. Jensen, Chem. Eng. Sci. 56 (2001) 293-303.
[65]V. Hessel, H. Löwe, Chem Eng Technol 26 (2003) 13-24.
[66]Y. Pan, M. Ju, J. Yao, L. Zhang, N. Xu, Chem. Commun. (2009) 7233-7235.
[67]T. Wakihara, R. Ichikawa, J. Tatami, A. Endo, K. Yoshida, Y. Sasaki, K. Komeya, T. Meguro, Cryst. Growth Des. 11 (2011) 955-958.
[68]Ch. Baerlocher, L.B. Mccusker, Database of Zeolite Structures
http://www.iza-structure.org/databases/.

[69]F.G. Delprato, J.-L.; Anglerot, D.; Zivkov, C, Eur. Pat. 364352, 1990.
[70]G. Lischke, E. Schreier, B. Parlitz, I. Pitsch, U. Lohse, M. Woettke, Appl. Catal., A 129 (1995) 57-67.
[71]A. Haas, D.A. Harding, J.R.D. Nee, Microporous Mesoporous Mater. 28 (1999) 325-333.
[72]E.-P. Ng, H. Awala, K.-H. Tan, F. Adam, R. Retoux, S. Mintova, Microporous Mesoporous Mater. 204 (2015) 204-209.
[73]Y. Wang, J. Zhang, X. Meng, S. Han, Q. Zhu, N. Sheng, L. Wang, F.-S. Xiao, Microporous Mesoporous Mater. 286 (2019) 105-109.
[74]V.P. Valtchev, K.N. Bozhilov, J. Phys. Chem. B 108 (2004) 15587-15598.
[75]Y. Huang, K. Wang, D. Dong, D. Li, M.R. Hill, A.J. Hill, H. Wang, Microporous Mesoporous Mater. 127 (2010) 167-175.
[76]Y. Wang, M. Fan, L. Zhu, S. Wang, Y. He, Q. Li, Chem Res Chin Univ 35 (2019) 449-456.
[77]G. Majano, A. Darwiche, S. Mintova, V. Valtchev, Ind. Eng. Chem. Res. 48 (2009) 7084-7091.
[78]L. Chen, T. Xue, H. Wu, P. Wu, RSC Adv. 8 (2018) 2751-2758.
[79]S. Laurent, E.P. Ng, C. Thirifays, L. Lakiss, G.M. Goupil, S. Mintova, C. Burtea, E. Oveisi, C. Hébert, M. De Vries, M.M. Motazacker, F. Rezaee, M. Mahmoudi, Toxicol Res-Uk 2 (2013) 270-279.
[80]R. Li, N. Linares, J.G. Sutjianto, A. Chawla, J. Garcia-Martinez, J.D. Rimer, Angew. Chem. Int. Ed. 57 (2018) 11283-11288.
[81]X. Zhou, Y. Chen, T. Ge, Z. Hua, H. Chen, J. Shi, Sci. Bull. 62 (2017) 1018-1024.
[82]H. Zhang, H. Zhang, P. Wang, Y. Zhao, Z. Shi, Y. Zhang, Y. Tang, RSC Adv. 6 (2016) 47623-47631.
[83]C. Minkowski, R. Pansu, M. Takano, G. Calzaferri, Adv. Funct. Mater. 16 (2006) 273-285.
[84]V. Vohra, A. Bolognesi, G. Calzaferri, C. Botta, Langmuir 25 (2009) 12019-12023.
[85]A.G. Mohammad S, N.H. Ahmad, K. Goldyn, S. Mintova, T.C. Ling, E.-P. Ng, Mater Res Express 6 (2018) 025026.
[86]S. Chen, L.P. Sorge, D.-K. Seo, Nanoscale 9 (2017) 18804-18811.
[87]S.-F. Wong, H. Awala, A. Vincente, R. Retoux, T.C. Ling, S. Mintova, R.R. Mukti, E.-P. Ng, Microporous Mesoporous Mater. 249 (2017) 105-110.
[88]E.-P. Ng, G.K. Lim, G.-L. Khoo, K.-H. Tan, B.S. Ooi, F. Adam, T.C. Ling, K.-L. Wong, Materials Chemistry and Physics 155 (2015) 30-35.
[89]M. Haouas, L. Lakiss, C. Martineau, J. El Fallah, V. Valtchev, F. Taulelle, Microporous Mesoporous Mater. 198 (2014) 35-44.
[90]Y.-W. Cheong, K.-L. Wong, T.C. Ling, E.-P. Ng, Materials Express 8 (2018) 463-468.
[91]J. Grand, N. Barrier, M. Debost, E.B. Clatworthy, F. Laine, P. Boullay, N. Nesterenko, J.-P. Dath, J.-P. Gilson, S. Mintova, Chem. Mater. 32 (2020) 5985-5993.
[92]M. Rahimnejad, S.K. Hassaninejad-Darzi, S.M. Pourali, Journal of the Iranian Chemical Society 12 (2015) 413-425.
[93]S.T. Wilson, B.M. Lok, C.A. Messina, T.R. Cannan, E.M. Flanigen, J. Am. Chem. Soc. 104 (1982) 1146-1147.
[94]R.E. Morris, Chem. Commun. (2009) 2990-2998.
[95]Z. Ma, J. Yu, S. Dai, Adv. Mater. 22 (2010) 261-285.
[96]E.-P. Ng, L. Itani, S.S. Sekhon, S. Mintova, Chem. Eur. J. 16 (2010) 12890-12897.
[97]Y. Shi, X. Zhang, L. Wang, G. Liu, Materials Letters 124 (2014) 212-214.
[98]L. Gopal, G.K. Lim, T.C. Ling, R. Adnan, J.C. Juan, E.-P. Ng, Materials Letters 182 (2016) 344-346.

[99]D. Fan, N. Barrier, A. Vicente, J.-P. Gilson, S. Clevers, V. Dupray, G. Coquerel, V. Valtchev, Inorg. Chem. Front. 7 (2020) 542-553.
[100] S.L. Suib, Acc. Chem. Res. 41 (2008) 479-487.
[101] Y.F. Shen, R.P. Zerger, R.N. Deguzman, S.L. Suib, L. Mccurdy, D.I. Potter, C.L. Young, Science 260 (1993) 511.
[102] R.N. De Guzman, A. Awaluddin, Y.-F. Shen, Z.R. Tian, S.L. Suib, S. Ching, C.-L. O'young, Chem. Mater. 7 (1995) 1286-1292.
[103] J. Yuan, K. Laubernds, Q. Zhang, S.L. Suib, J. Am. Chem. Soc. 125 (2003) 4966-4967.
[104] X.F. Shen, Y.S. Ding, J. Liu, J. Cai, K. Laubernds, R.P. Zerger, A. Vasiliev, M. Aindow, S.L. Suib, Adv. Mater. 17 (2005) 805-809.
[105] R.N. De Guzman, Y.F. Shen, B.R. Shaw, S.L. Suib, C.L. O'young, Chem. Mater. 5 (1993) 1395-1400.
[106] J. Yuan, W.-N. Li, S. Gomez, S.L. Suib, J. Am. Chem. Soc. 127 (2005) 14184-14185.
[107] J. Yuan, K. Laubernds, J. Villegas, S. Gomez, S.L. Suib, Adv. Mater. 16 (2004) 1729-1732.
[108] H. Huang, S. Sithambaram, C.-H. Chen, C. King'ondu Kithongo, L. Xu, A. Iyer, H.F. Garces, S.L. Suib, Chem. Mater. 22 (2010) 3664-3669.
[109] S. Dharmarathna, C.K. King'ondu, W. Pedrick, L. Pahalagedara, S.L. Suib, Chem. Mater. 24 (2012) 705-712.
[110] S. Mintova, J. Grand, V. Valtchev, Comptes Rendus Chimie 19 (2016) 183-191.
[111] T. Kuzniatsova, Y. Kim, K. Shqau, P.K. Dutta, H. Verweij, Microporous Mesoporous Mater. 103 (2007) 102-107.
[112] A. Jawor, B.-H. Jeong, E.M.V. Hoek, Journal of Nanoparticle Research 11 (2009) 1795.
[113] M. Rahimi, E.P. Ng, K. Bakhtiari, M. Vinciguerra, H.A. Ahmad, H. Awala, S. Mintova, M. Daghighi, F. Bakhshandeh Rostami, M. De Vries, M.M. Motazacker, M.P. Peppelenbosch, M. Mahmoudi, F. Rezaee, Sci. Rep. 5 (2015) 17259.
[114] D.J. Wales, J. Grand, V.P. Ting, R.D. Burke, K.J. Edler, C.R. Bowen, S. Mintova, A.D. Burrows, Chem. Soc. Rev. 44 (2015) 4290-4321.